

ALTERNATIVE APPROACHES FOR TRANSIENT-FLOW LABORATORY-SCALE PERMEAMETRY

Michael J. Hannon, Jr.
The University of Alabama at Birmingham

This paper was prepared for presentation at the International Symposium of the Society of Core Analysts held in Snowmass, Colorado, USA, 21-26 August 2016

ABSTRACT

Although pressure-pulse-decay permeametry has been in wide use for the past 50 years, its standard configuration and design have remained largely intact, with performance optimizations based mostly on sample geometry and reservoir volumes. For characterizing ultra-low permeability materials like shales or caprocks, where the pulse-decay methodology often becomes problematic, many have turned to unsteady-state analyses on crushed fragments. A paucity of models exists in the public literature for the latter scenario, most of which are analytical approximations of very simple cases. This study addresses both issues by proposing analytical flow models for alternative experimental schemes. First, new unidimensional flow scenarios are considered as substitutes for the classical pulse-decay techniques on cylindrical core samples. Such strategies can decrease testing times by more than an order of magnitude as compared to conventional pressure-pulse-decay strategies with similar fidelity. Second, a model is presented here that relaxes a key simplifying assumption inherent to publicly available models for crushed media, namely that the entire collection of particles is of uniform size. Rather, an analytical model for a discrete distribution of sizes is presented that more accurately represent the broad range of particle sizes that are typically seen in crushed materials.

INTRODUCTION

Site characterization of geologic formations begins with the collection of native core samples and their analysis by bench-top laboratory experiments. Although these analyses occur on a minute sample size with respect to the reservoirs under investigation, they are used as the “ground truth” against which field-scale data are calibrated. Perhaps nowhere is this approach more important than in the assessment of permeability. Conventional steady-state measurements performed on samples from highly porous and permeable storage formations provide accurate estimates of permeability in a reasonable amount of time. But for the ultra-tight formations interlaced between them, measuring permeability is much more difficult. The ability to perform such measurements in a way that is both reproducible and timely continues to elude interested parties, who require them for applications such as unconventional hydrocarbon recovery [1] or geological contaminant storage [2].

The most prevalent rapid permeametry techniques for shale and caprock materials are based upon the pressure-pulse-decay experimental scheme [3]. Offshoot approaches of this baseline strategy, most notably the pulse-decay analysis performed on crushed samples [4], provide estimates of very low permeability quite rapidly. But they do not always do so within a level of certainty that meets industry needs [5]. A technique that could resolve core-scale permeabilities reliably in a reasonable amount of time would be a significant technological leap forward. As a step in that direction, this report considers alternative approaches to the standard pressure-pulse decay on cylindrical core samples and an additional flow model for pulses applied to crushed media.

ALTERNATIVE FLOW SCENARIOS

To address many of the limitations inherent to the models outlined in the current art, this section considers alternative unidimensional flow scenarios which can be reduced to analytical models. It begins by describing slight modifications to the classical techniques involving flow along the axial direction of cylindrical core samples, followed by models for flow in the radial direction of cylindrical specimens. These approaches could form baseline alternatives to the industry-standard pulse-decay. The most prevalent of these variant approaches is crushed-core transient-flow permeametry, which has a shortage of publicly available flow models to compare against its experimental data. Toward that end, a model is presented for a pulse applied to a discrete size distribution of porous spherical particles.

In order to linearize the governing equations in the presence of changing fluid viscosity μ , compressibility c , and compressibility factor Z , the pressure variable p and temporal variable t were transformed to the pseudo-pressure (p^*) and pseudo-time (t^*) domains defined in Equations 1 and 2, respectively [6].

$$p^* \equiv \int_{p_i}^p \frac{p'}{\mu(p')Z(p')} dp'; \quad dp^* = \frac{p}{\mu Z} dp \quad (1)$$

$$t^* \equiv (\mu c)_{ref} \int_0^t \frac{dt'}{\mu(p(x, t'))c(p(x, t'))}; \quad dt^* = \frac{(\mu c)_{ref}}{\mu c} dt \quad (2)$$

The subscript “ref” denotes properties evaluated at a reference condition, such as their average values over the duration of the test. The dependent variable is non-dimensionalized to its final form p_D^* by the pseudo-pressure evaluated under pulse conditions p_p^* (i.e., $p_D^* \equiv p^*/p_p^*$) and the independent temporal variable is normalized by the time constant τ_ℓ (i.e., $t_{D,\ell}^* \equiv t^*/\tau_\ell$). Defined by Eq. 3, this time constant depends on the thermo-physical properties of the permeant $(\mu c)_{ref}$, the length scale of each scenario ℓ , the porosity of the sample ϕ , and the apparent permeability k (assumed constant) of the sample to the gaseous permeant under the pressure conditions of a given experiment.

$$\tau_\ell \equiv \frac{\phi(\mu c)_{ref} \ell^2}{k} \quad (3)$$

Axial Flow in Cylindrical Samples ($\ell = L$)

One slight change to the standard pressure-pulse decay would be to apply a step disturbance in both reservoirs (having volumes V_0 and V_1) simultaneously, as shown in Figure 1. By doing so, the time required for the system to reach equilibrium decreases significantly. A four-fold decrease in time can be attributed to effectively cutting the characteristic length scale (in this case, chosen as the sample length L) in half (see Equation 3), and equilibration no longer requires filling the downstream reservoir. Figure 1 provides example pressure responses to a simultaneous pulse applied to both ends of a homogenous sample with apparatuses having various reservoir volumes ($\gamma_0 \equiv V_0/V_p$, $\gamma_1 \equiv V_1/V_p$, where V_p indicates the pore volume of the sample).

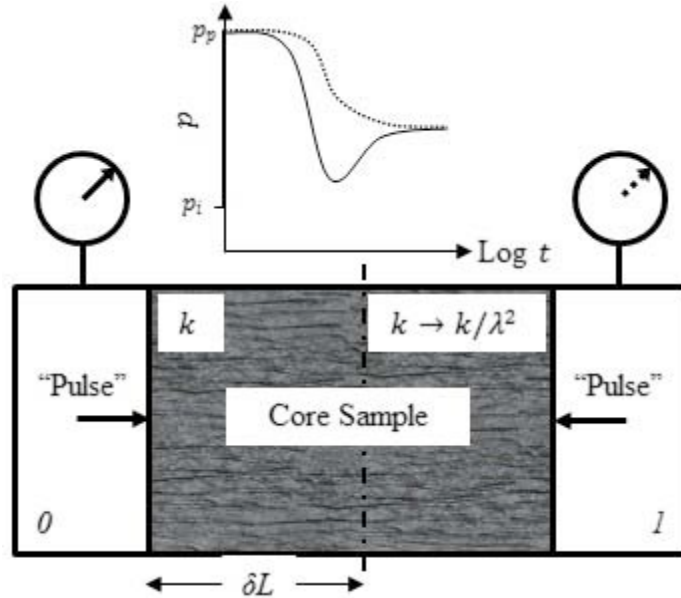


Figure 3. Schematic of a bi-directional pressure-pulse-decay model for a sample having a discrete discontinuity of permeability at a distance δL from the upstream face.

Applying a simultaneous pressure increase in both reservoirs also enables a rapid characterization of core-scale longitudinal heterogeneity [7] from a single test. Toward

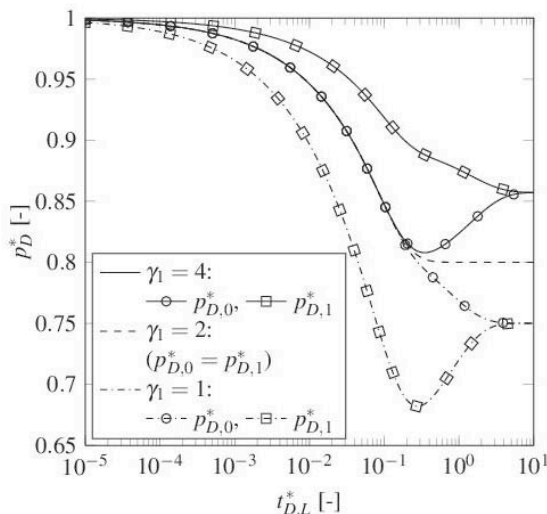


Figure 1. Bidirectional pressure-pulse decay of a homogeneous sample (i.e., $\lambda^2 = 1$) with one reservoir-volume ratio fixed ($\gamma_0 = 2$) and the other (γ_1) variable.

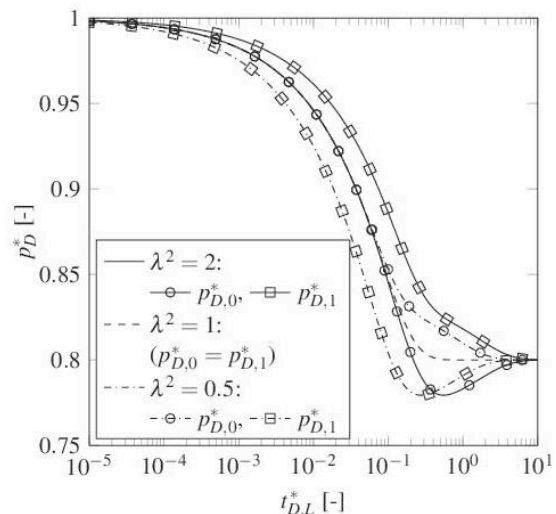


Figure 2. Bidirectional pressure-pulse decay with fixed reservoir volumes ($\gamma_0 = \gamma_1 = 2$) of a heterogeneous sample with varying permeability ratio λ^2 and fixed discontinuity location ($\delta = 0.5$).

that end, an analytical solution for the case of a discrete permeability discontinuity imposed at an arbitrary plane (located a distance δL from the upstream face) within a sample having uniform porosity is presented in Figure 2.

Radial Flow in Cylindrical Samples ($\ell = R$)

Another technique for decreasing the length of the flow path for the permeant, and therefore the equilibration time, is to invert the normal pulse-decay apparatus by sealing the circular ends of a cylindrical sample and allowing the fluid to infiltrate its circumferential surface (Figure 4). The underlying assumption here is a uniform-permeability fabric along the radial direction r of the sample. At the core scale, this is reasonable for many varieties of lithologic samples extracted perpendicular to their native bedding planes under uniform radial confining stress, which is the only stress state achievable in cylindrical core-holder apparatuses. Figure 5 shows pressure-response curves from the outer reservoir ($p_D^*|_{r=R}$) and along the sample centerline ($p_D^*|_{r=0}$), plotted for various reservoir volumes ($\gamma \equiv V/V_p$, where V is the volume of the reservoir). Although the latter of these pressures could not be measured directly, they are shown here to indicate equilibration of the system.

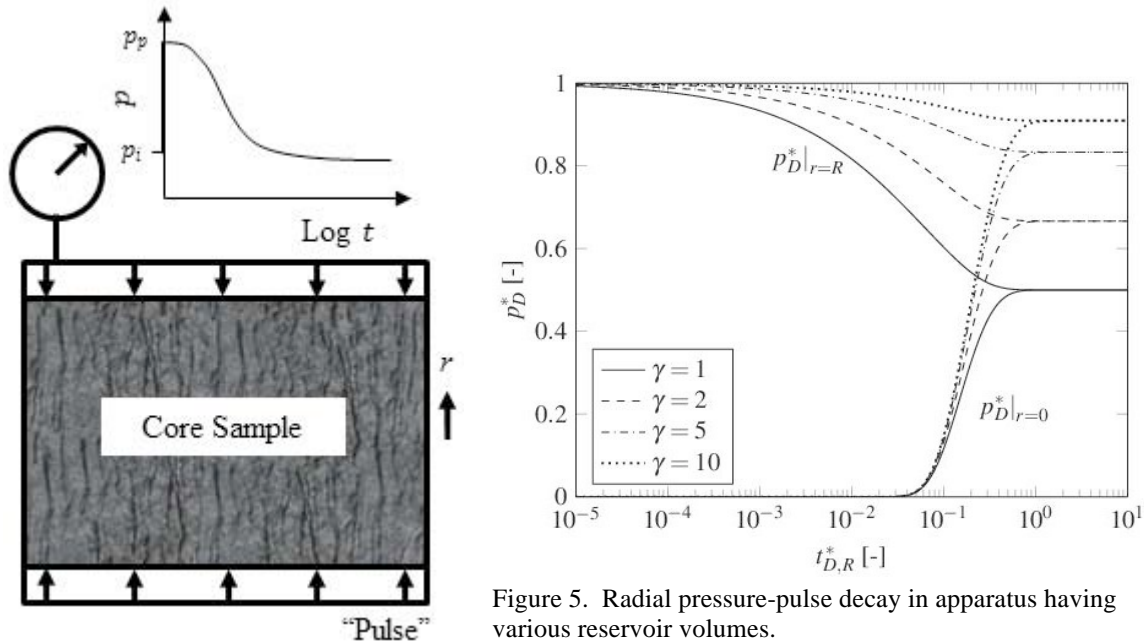


Figure 4. Schematic of a radially oriented pressure-pulse-decay experiment.

Radial Flow in a Discrete Size Distribution of Spherical Particles ($\ell = R_{eq}$)

Publicly available models predicting the pressure response from pulse-decay tests on crushed particles assume them to be a collection of uniformly sized homogeneous, isotropic spheres [8]. While this may be a suitable approach for a select portion of crushed materials (such as those collected from a single sieve layer), permeability estimates are known to decrease with decreasing particle size [4]. To analyze a wider

array of particle sizes, an analytical model was generated for a pressure disturbance applied to a collection of spherical particles having a discrete distribution of M different sizes, the i^{th} of which has particles of radius R_i and contains fraction χ_i of the overall volume (or mass, assuming constant grain density) of the particles. The characteristic length is chosen as the equivalent radius R_{eq} of a single sphere having identical volume as the entire collection of particles. Pressure-decay curves from these solutions are plotted in Figure 6 for a discrete particle size distribution comparable to those typically seen in industry, as given in Table 1.

Table 1. Typical particle size distribution for crushed shale samples, provided by Weatherford International, Ltd. (personal communication, 2015).

Sieve Size	χ_i [%]	R_i [mm]
>60	9.20	0.088
60	5.47	0.177
35	6.73	0.324
20	29.4	0.594
12	21.7	0.996
8	27.5	1.53

$$\bar{R} = \sqrt[3]{\sum_{i=1}^M \chi_i R_i^3} = 1.08 \text{ mm}$$

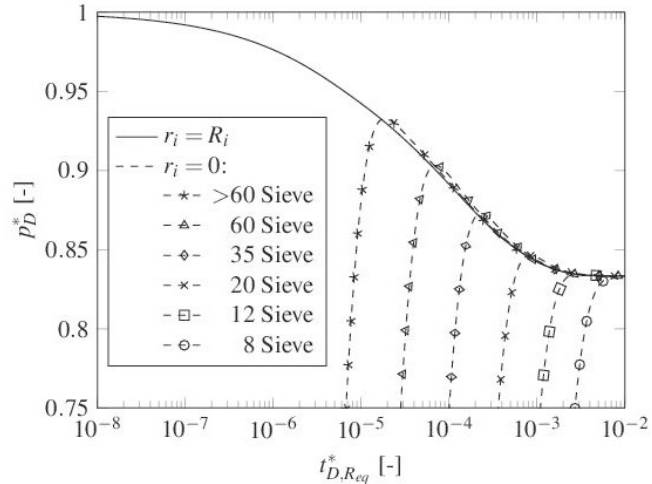


Figure 6. Pressure-pulse decay for a distribution of spherical particles collected from a cylindrical core having diameter equal its length, partitioned in a typical sieve-size distribution (Table 1) in a typical reservoir volume ($\gamma = 5$).

COMPARISONS AMONG EXPERIMENTAL SCHEMES

Error! Reference source not found. shows the anticipated pressure responses from the multiple pulse-decay techniques discussed previously, based on a homogeneous,

Table 2. Comparison of the times required by each flow condition demonstrated in Figure 11 to decay the pressure disturbance to within 0.01% of equilibrium. The “crushed” case indicates the pressure response to a pulse applied to spherical particles collected by crushing the same cylindrical plug into the size distribution of particles described in Table 1.

Experiment	$t_{D,L}^*$	\times Faster
Unidirectional	5.17	1.0
Bidirectional	0.665	7.77
Radial	0.294	17.6
Crushed	0.00203	2,550

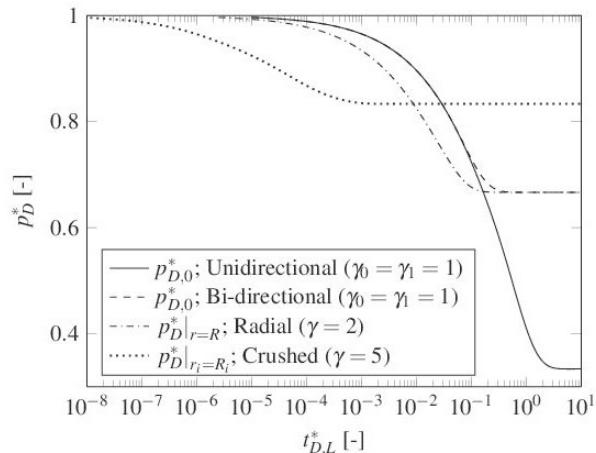


Figure 7. Comparison of various unsteady-state permeametry methodologies based on a cylindrical sample having diameter equal to its length.

cylindrical sample having a diameter equal to its length. **Error! Reference source not found.** compares the amount of time necessary for the pressure disturbance to decay to within 0.01% of its final equilibrium value for each experimental scheme, with similar comparisons noted for various stages of partial equilibrium. Reservoir sizes (provided in the legend of **Error! Reference source not found.**) were selectively chosen to draw appropriate comparisons among the various experimental schemes. The bi-directional- and radial-flow cases would provide more than a 7.5- and 17.5-fold reduction, respectively, in test time compared to the conventional approach. These benefits come at the cost of a more limited range on the observed pressure response, but transducers are available having sufficiently high precision to provide satisfactory measurements over this range. A much faster (>2,500×) reduction in equilibration time is noted from the crushed-sample approach, but it has well-documented limitations in the accuracy of its permeability estimates [5]. The bi-directional and radial transient-flow schemes provide means for low-permeability assessment with a combination of speed, reliability and representativeness far more practical to many industrial applications.

ACKNOWLEDGEMENTS

This work was supported by the U.S. National Energy Technology Laboratory. It summarizes a manuscript currently in review by *Transport in Porous Media*.

REFERENCES

1. Chhatre, S.S., Braun, E.M., Sinha, S., Passey, Q.R., Zirkle, T.E., Wood, A.C., Boros, J.A., Berry, D.W., Leonardi S.A., and Kudva, R.A., "Steady state permeability measurements of tight oil bearing rocks," SCA 2014-12.
2. Hannon, Jr., M.J. and Esposito, R.A., "Screening considerations for caprock properties in regards to commercial-scale carbon-sequestration operations," *International Journal of Greenhouse Gas Control*, (2015) **32**, pp. 213-223.
3. Brace, W.F., Walsh, J.B., and Frangos, W.T., "Permeability of granite under high pressure," *Journal of Geophysical Research*, (1968) **73**, 6, pp. 2225-2236.
4. Luffel, D.L., "Advances in shale core analysis," Technical Report GRI-93/0297, Gas Research Institute, 1993.
5. Spears, R.W., Dudus, D., Foulds, A., Passey, Q.R., Sinha, S., and Esch, W.L., "Shale gas core analysis: strategies for normalizing between laboratories and a clear need for standard materials," SPWLA-2011-A, presented at the 52nd Annual Logging Symposium, 2011.
6. Haskett, S.E., Narahara, G.M., and Holditch, S.A., "A method for simultaneous determination of permeability and porosity in low-permeability cores," *SPE Formation Evaluation*, (1988) **3**, 3, pp. 651-658.
7. Kamath, J., Boyer, R.E., and Nakagawa, F.M., "Characterization of core scale heterogeneities using laboratory pressure transients," *SPE Formation Evaluation*, (1992) **7**, 3, pp. 219-227.

8. Profice, S., Lasseux, D., Jannot, Y., Jebara, N., and Hamon, G., "Permeability, porosity and Klinkenberg coefficient determination on crushed porous media," SCA 2011-32.